Biochem. Soc. Symp. **74**, 9–22
(Printed in Great Britain)

2

The IP_3 receptor/Ca^{2+} channel and its cellular function

Katsuhiko Mikoshiba[1]

Division of Molecular Neurobiology, The Institute of Medical Science, The University of Tokyo, 4-6-1 Shirokanedai, Minato-ku, Tokyo 108-8639, Japan, Laboratory for Development Neurobiology, Brain Science Institute, RIKEN, 2-1 Hirosawa, Wako, Saitama 351-0198, Japan, and Calcium Oscillation Project, ICORP-SORST, Japan Science and Technology Agency, 4-1-8 Hon-cho, Kawaguchi, Saitama 332-0012, Japan

Abstract

The IP_3R [IP_3 (inositol 1,4,5-trisphosphate) receptor] is responsible for Ca^{2+} release from the ER (endoplasmic reticulum). We have been working extensively on the P_{400} protein, which is deficient in Purkinje-neuron-degenerating mutant mice. We have discovered that P_{400} is an IP_3R and we have determined the primary sequence. Purified IP_3R, when incorporated into a lipid bilayer, works as a Ca^{2+} release channel and overexpression of IP_3R shows enhanced IP_3 binding and channel activity. Addition of an antibody blocks Ca^{2+} oscillations indicating that IP_3R1 works as a Ca^{2+} oscillator. Studies on the role of IP_3R during development show that IP_3R is involved in fertilization and is essential for determination of dorso-ventral axis formation. We found that IP_3R is involved in neuronal plasticity. A double homozygous mutant of IP_3R2 (IP_3R type 2) and IP_3R3 (IP_3R type 3) shows a deficit of saliva secretion and gastric juice secretion suggesting that IP_3Rs are essential for exocrine secretion. IP_3R has various unique properties: cryo-EM (electron microscopy) studies show that IP_3R contains multiple cavities; IP_3R allosterically and dynamically changes its form reversibly (square form–windmill form); IP_3R is functional even though it is fragmented by proteases into several pieces; the ER forms a meshwork but also forms vesicular ER and moves along microtubules using a kinesin motor; X ray analysis of the crystal structure of the IP_3 binding core consists of an N-terminal β-trefoil domain and a C-terminal α-helical domain. We have discovered ERp44 as a redox sensor in the ER which binds to the luminal part of IP_3R1 and regulates its activity. We have also found the role of IP_3 is not only to release Ca^{2+} but also to release IRBIT which binds to the IP_3 binding core of IP_3R.

[1]email mikosiba@ims.u-tokyo.ac.jp

Introduction

IP_3 (inositol 1,4,5-trisphosphate) is a second messenger produced through phosphoinositide turnover in response to various extracellular stimuli such as hormones, growth factors, neurotransmitters, neutrophins, odorants and light. IP_3 induces Ca^{2+} release from intracellular Ca^{2+} store sites, such as the ER (endoplasmic reticulum). The IP_3R (IP_3 receptor) is an IP_3-gated Ca^{2+} release channel and could be considered as a signal converter that converts IP_3 signals into Ca^{2+} signals and plays an important role in controlling a variety of Ca^{2+}-dependent cellular functions (cell proliferation, differentiation, fertilization, embryonic development, secretion, muscular contraction, immune responses, brain functions, chemical sense, light transduction, etc.) Our goal is to elucidate the structure–function relationship of the IP_3R and the physiological roles of IP_3R-mediated Ca^{2+} signalling in various cell types.

Discovery of IP_3R

IP_3 was found to release Ca^{2+} from intracellular stores [1]. However, the Ca^{2+} store had only previously been reported as a non-mitochondrial store, and it was not known whether the IP_3R was an IP_3-binding protein or whether the IP_3R was a Ca^{2+} release channel. Many researchers were searching for the target molecule of IP_3 [2,3]. We have been working on the P_{400} protein, the expression of which increases during development and is almost absent in the cerebellar mutant mice where Purkinje cells are deficient or spines of Purkinje cells are absent [4–6]. We have discovered that P_{400} protein is an IP_3R-binding protein and we have determined the whole primary sequence [7,8]. IP_3R works as a channel by incorporating the purified IP_3-binding protein into lipid bilayers [9]. Purified IP_3R incorporated into liposomes express Ca^{2+} releasing activity [10,11]. Overexpression of IP_3R1 enhances both IP_3-binding activity and also Ca^{2+} releasing activity [12]. All these data indicate that IP_3R is an IP_3-gated Ca^{2+} release channel.

Role of IP_3R in development and neural plasticity

IP_3R1 (type 1 IP_3R) plays a role in determination of dorso-ventral axis formation

Dorso-ventral axis formation is an essential step for the body plan. Early in embryonic growth, the signalling pathway specifies the development pattern. Evidence has been obtained that blockage of PtdIns turnover in the ventral part of the embryo by injecting lithium chloride leads to the conversion of the ventral mesoderm into the dorsal mesoderm, thereby generating ectopic dorsal axes. Injection of the functional blocking antibody against IP_3R converts ventral mesoderm into dorsal mesoderm. This finding suggests a role for the IP_3/Ca^{2+} signalling pathway as a ventralizing signal in addition to the already known pathway through glycogen synthase kinase 3β [13]. We found that a downstream target of the IP_3R is NFAT (nuclear factor of activated T-cells).

The dominant-negative form of NFAT converts ventral mesoderm into dorsal mesoderm [14].

IP_3R1 is involved in neurite extension

It has been shown using micro-CALI (chromophore-assisted laser inactivation), a process that uses a laser beam to irradiate an antibody labelled with a dye, that IP_3Rs could be inactivated. This procedure provided important clues concerning the outgrowth of the neuronal axon. Experiments suggest that Ca^{2+} release mediated by the IP_3R is deeply involved in neurite extension [15].

IP_3R1 is involved in neuronal plasticity [LTD (long term depression) in the cerebellum and LTP (long term potentiation) in the hippocampus]

The IP_3R acts as an IP_3-gated Ca^{2+} release channel in a variety of cell types. IP_3R1 is the major neuronal member of the IP_3R family in the central nervous system. We found that most IP_3R1-deficient mice, generated by gene targeting, die *in utero*, and animals that are born have severe ataxia and tonic or tonic–clonic seizures and die by the weaning period. Electroencephalograms have shown that they suffer from epilepsy, indicating that IP_3R1 is essential for proper brain function [16]. We found that the IP_3R-deficient mice could be used as valuable model animals in studying the role of the IP_3R in neuronal plasticity.

Since the IP_3R is highly enriched in Purkinje neurons in the cerebellum, a test was conducted as to whether LTD, involving the cerebellar memory system is altered or not in the IP_3R-deficient mice. Purkinje neurons from the IP_3R-deficient mice and those injected with the anti-IP_3R antibody showed a blockage of LTD, suggesting the importance of the IP_3R in cerebellar plasticity [17]. We then studied LTP in hippocampal slices of IP_3R1-deficient mice. LTP of CA1 hippocampus of the IP_3R1-deficient mice showed no significant difference from that of wild-type by standard tetanus. LTP was induced by short tetanus only in the mutant. LTD at CA1 hippocampus was induced by short low-frequency stimuli in both the wild-type and the mutant. Depotentiation of LTP after standard tetanus was observed in the wild-type, but the depotentiation was abolished in the mutant [18]. Low-frequency stimuli induced LTD but the LTD suppressed subseqent LTP induced by standard tetanus (LTP suppression). The LTP suppression was abolished in the mutant [18,19]. Furthermore, we found that IP_3R1 was involved in the determination of polarity and input specificity of synapse [20]. These data clearly show that the IP_3R is involved in development and neuronal plasticity.

Structure and function of IP_3Rs

We have cloned three types of human and mouse IP_3R (IP_3R1, IP_3R2 and IP_3R3) [21–22] and have analysed the structure and function of each type of IP_3R by means of molecular biological, biochemical, cell biological, physiological and histochemical approaches. We have found that each type has different IP_3-binding (e.g. affinity, specificity and Ca^{2+} sensitivity) and modulation (e.g. phosphorylation and calmodulin-binding) properties. The IP_3R

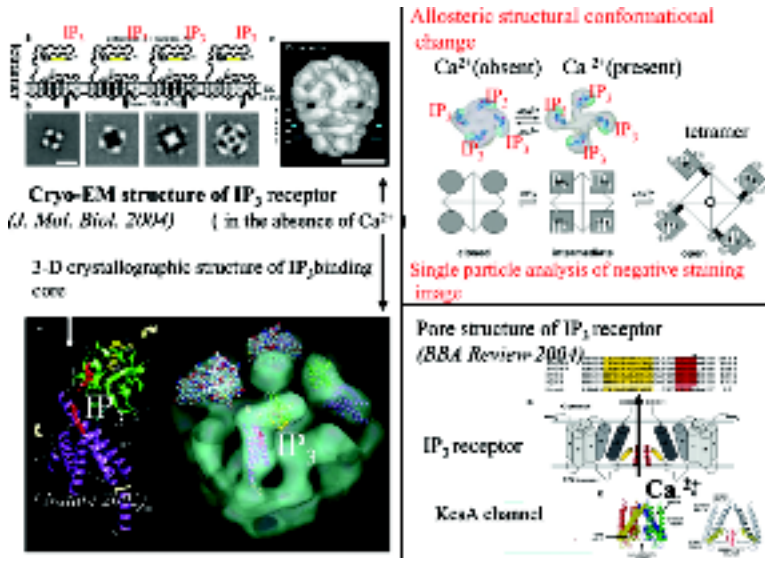

Figure 1 Three-dimensional structure of the IP_3R. Left panel: cryo-EM structure of IP_3R. X-ray three-dimensional structure of the IP_3 binding core (lower left) is aligned to the L shaped part of the IP_3R (lower right). (**b**, **e** and **h**) It is clear from the section of cryo-EM structure that there is a cavity inside and there are many pores on the balloon-like surface [28]. Right panel: EM figure of the IP_3R by negative staining demonstrating its allosteric structural change in the absence (**a**) and presence (**b**) of Ca^{2+} [26,27]. The pore structure of the IP_3 receptor is similar to the KcsA channel [28a]. Top left-hand panel reproduced from *Journal of Molecular Biology,* vol. **336,** Sato, C., Hamada, K., Ogura, T., Miyazawa, A., Iwasaki, K., Hiroaki, Y., Tani, K., Terauchi, A., Fujiyoshi, Y. and Mikoshiba, K., Inositol 1,4,5-trisphosphate receptor contains multiple cavities and L-shaped ligand-binding domains, 155–164, Copyright (2004), with permission from Elsevier. Bottom left-hand panel reproduced with permission from Macmillan Publishers Ltd: *Nature* (2002) vol. **420,** pages 696–700; Copyright (2002). Bottom right-hand panel reproduced from *Biochimica et Biophysica Acta*, vol. **1742,** Bosanac, I., Michikawa, T., Mikoshiba, K. and Ikura, M., Structural insights into the regulatory mechanism of IP3 receptor, 89–102, Copyright (2004), with permission from Elsevier.

(Figure 1) is a polypeptide (approx. 2700 amino acids) with five major functionally distinct domains: (i) the N-terminal IP_3-binding suppressor/coupling domain; (ii) the IP_3-binding domain; (iii) the central modulatory/coupling domain; (iv) the channel-forming domain; and (v) the C-terminal gate-keeper domain [22a]. Four IP_3R subunits assemble to form a functional IP_3-gated Ca^{2+} release channel and both homo- and hetero-tetrameric channels are detected. IP_3R possesses six transmembrane segments, suggesting that IP_3R shares a basic design of the channel-forming domain with the voltage-gated and second-messenger-gated ion channels on the plasma membrane [22a]. We analysed the folding structure of the IP_3R channel by limited trypsin digestion and found that the IP_3R channel is an assembly of four subunits, each of which is constituted by non-covalent interactions of five major well-folded structural components [22b]. The IP_3-binding core, a minimum essential region for specific IP_3 binding, resides among residues

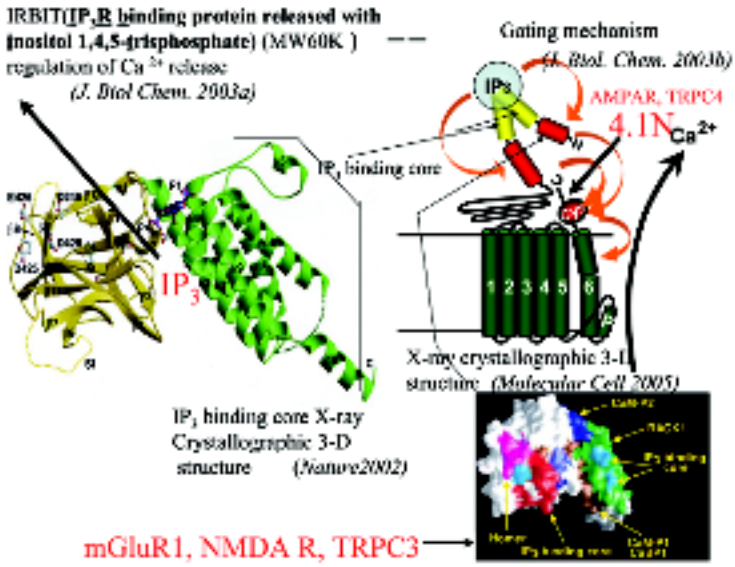

Figure 2 The N-terminal ligand binding site associates with the C-terminal region and works as a hot spot for the regulation of IP_3R function. Reproduced with permission from Macmillan Publishers Ltd: *Nature* (2002) vol. **420,** pages 696–700; Copyright (2002). Reproduced from Molecular Cell, vol. **17,** Bosanac, I., Yamazaki, H., Matsu-ura, Michikawa, T., Mikoshiba, K. and Ikura, M., Crystal structure of the ligand binding suppressor domain of type 1 inositol 1,4,5-trisphosphate receptor, 193–2003, Copyright (2005), with permission from Elsevier.

226–578 of mouse IP_3R1. The N-terminal 220 residues directly preceding the IP_3-binding core domain play a key role in IP_3-binding suppression and partner protein interaction [22a] (see Figure 2).

X-ray crystallographic studies of the three-dimensional structure of the IP_3-binding core

Previously, we have uncovered crystal structures of both the IP_3-binding core in complex with IP_3 and the suppressor domain of mouse IP_3R1 at 2.2 Å (1Å=0.1 nm) and 1.8 Å resolutions respectively (Figure 2) [24,25]. The IP_3-binding core forms the asymmetric boomerang-like structure consisting of an N-terminal β-trefoil domain and a C-terminal α-helical domain containing an armadillo-repeat-like fold. The cleft formed by the two domains exposes a cluster of arginine and lysine residues that co-ordinate the three phosphoryl groups of IP_3 [22a,28a]. Displaying a shape akin to a hammer, the suppressor region contains a 'head' subdomain forming the β-trefoil fold and an 'arm' subdomain possessing a helix–turn–helix structure that protrudes from the globular head subdomain. Site-directed mutagenesis studies provide evidence for the involvement of a large conserved surface area on the head subdomain in the suppression of IP_3 binding to the IP_3-binding core domain. This conserved region is in close proximity to the previously proposed binding sites of Homer, RACK1, calmodulin and CaBP1 [25].

Allosteric structural changes of IP_3R

Ca^{2+} signalling often exhibits dynamic changes in time and space inside a cell (known as Ca^{2+} waves and Ca^{2+} oscillations). These complex spatiotemporal patterns are not produced by simple diffusion of cytoplasmic Ca^{2+}. The essential ingredients to generate repetitive Ca^{2+} spikes are positive feedback, co-operativity, deactivation (including negative feedback) and reactivation. The IP_3R1 is regulated by cytoplasmic Ca^{2+} in a biphasic manner with a maximal channel activity at 200–500 nM cytoplasmic Ca^{2+}. We found that the positive feedback regulation by cytoplasmic Ca^{2+} is an intrinsic property of the IP_3R1, whereas the negative feedback regulation by Ca^{2+} is mediated by calmodulin, a ubiquitous and multifunctional Ca^{2+}-dependent regulator protein. Ca^{2+} induces marked structural changes in the tetrameric IP_3R1 purified from mouse cerebella. Electron microscopy of the IP_3R1 particles revealed two distinct structures with 4-fold symmetry: a windmill-like structure and a mushroom-like structure. Ca^{2+} reversibly promotes a transition from the mushroom-like structure to the windmill-like structure with relocations of four peripheral IP_3-binding domains [26,27]. The effective concentration of Ca^{2+} for conformational changes in IP_3R1 is <100 nM. These data suggest that the Ca^{2+}-specific conformational change structurally regulates the IP_3-gated channel opening within the IP_3R.

Cryo-EM (electron microscopy)

We analysed the three-dimensional structure of the ligand-free form of IP_3R1 purified from mouse cerebella based on a single particle technique using an originally developed electron microscope equipped with a helium-cooled specimen stage and an automatic particle picking system. The shape of the density map obtained at 15 Å resolution is reminiscent of a hot air balloon, with the spherical cytoplasmic domain (diameter of 175 Å) representing the balloon and the square-shaped luminal domain (side length of 96 Å) representing the basket [28]. The structure of the density map consists of two layers. The outer hot-air-balloon-shaped shell forms many holes and cavities, whereas the inner shell is composed of a continuous square-shaped tubular density. The inner tubular density is slightly rotated in consecutive sections, revealing the inner tubule to be twisted. There is a prominent vacant space over the inner tubular density. The double-layered structure is shared between the IP_3R and voltage-gated Na^+ channels.

IP_3R dynamics in the ER membrane

Transport of IP_3R1 as vesicular ER on microtubules

The ER is considered to be a continuous meshwork structure. In addition to this, we have discovered another type of dynamic movement of the ER. Fluorescent-protein-tagged ER proteins were expressed in cultured mouse hippocampal neurons to monitor their movements using time-lapse microscopy. The vesicular ER moves rapidly along the dendrites in both anterograde and retrograted directions at a velocity of 0.2–0.3 μm/s. Depolymerization of microtubules, overexpression of dominant-negative kinesin, and kinesin depletion by antisense DNA reduced the number and velocity of the moving vesicles [29]. Vesicular ER is capable of taking

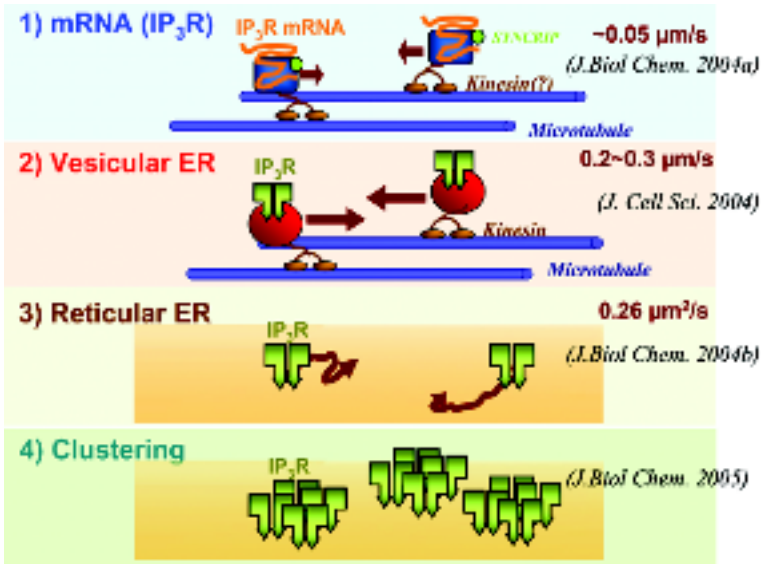

Figure 3 Four ways of intracellular trafficking of the IP_3R

up and releasing Ca^{2+} in addition to the reticular ER [29] (Figure 3). The rapid transport of the Ca^{2+}-releasable ER vesicles would contribute to the rapid supplying of fresh ER proteins to the dendrites of neurons, or to the spatial regulation of Ca^{2+} signalling inside the cell. In addition, mRNA granules which contain IP_3R1 mRNA are transported along the microtubules. It is interesting to know what kind of signals initiate translation and also to know where translation occurs inside the neuron.

IP_3R clustering in the ER membrane

It was reported that IP_3R forms clusters on the ER when cytoplasmic Ca^{2+} concentrations are elevated [22,22b]. However, molecular mechanism of IP_3R clustering remains largely unknown. We found that the time course of clustering of GFP–IP_3R1 (green-fluorescent-protein-tagged IP_3R1), evoked by IP_3-generating agonists, did not correlate with cytoplasmic Ca^{2+} concentrations but seemed to be compatible with cytoplasmic IP_3 concentrations. IP_3 production alone induced GFP–IP_3R1 clustering in the absence of a significant increase in Ca^{2+} concentration, but elevated Ca^{2+} concentration without IP_3 production did not. IP_3R1 mutants that did not undergo an IP_3-induced conformational change failed to form clusters. Thus IP_3R clustering is induced by its IP_3-induced conformational change to the open state.

Stimulation with ATP or Ca^{2+} ionophore induced cluster formation by all three types of recombinant mouse IP_3R expressed in COS-7 cells. We found that the size and shape of the stimulus-induced clusters differed among the three types of IP_3R, and IP_3R2 formed clusters even in the resting cell.

We found a novel alternative splicing segment, SI_{m2}, at residues 176–208 of IP_3R2. The long form ($IP_3R2\ SI_{m2}^+$) was dominant, but the short form ($IP_3R2\ SI_{m2}^-$) was detected in all tissues examined. $IP_3R2\ SI_{m2}^-$ has neither IP_3-binding activity nor Ca^{2+} releasing activity. $IP_3R2\ SI_{m2}^-$ does not form clusters in either resting or stimulated cells [22]. Co-expression of $IP_3R2\ SI_{m2}^-$ prevents stimulus-induced IP_3R clustering, suggesting that $IP_3R2\ SI_{m2}^-$ functions as a negative co-ordinator of stimulus-induced IP_3R clustering. Expression of $IP_3R2\ SI_{m2}^-$ in CHO-K1 cells significantly reduced ATP-induced Ca^{2+} entry, but not Ca^{2+} release, suggesting that the novel splice variant of IP_3R2 specifically influences the dynamics of the sustained phase of Ca^{2+} signals.

Identification and characterization of IP_3R-binding proteins

IP_3R has a unique structure (revealed by cryo-EM), which is convenient for interaction with many molecules. There are many molecules reported to interact with each other such as Huntingtin-associated protein 1 (HAP1A) [30], chromogranin A and B [31], CARP (carbonic anhydrase-related protein [32]), protein phosphatases (PP1 and PP2P) [30], cytoskeletal proteins such as Homer [33], 4.1N [34] and ankyrin [35], IRBIT (IP_3R-binding protein released with inositol 1,4, 5-trisphosphate) [36] and cytochrome C [37]. It is exciting to know that these molecules regulate the function of IP_3Rs.

IRBIT

We have found a novel protein, termed IRBIT, which interacts with IP_3R1 and was released upon IP_3 binding to IP_3R1 (Figure 4). IRBIT was purified from a high-salt extract of crude rat brain microsomes with IP_3 elution using an affinity column with the huge immobilized N-terminal cytoplasmic region of IP_3R1 (residues 1–2217) [36, 36a]. IRBIT, consisting of 530 amino acids, has a domain homologous with S-adenosylhomocysteine hydrolase at the C-terminal and a 104-amino-acid appendage containing multiple potential phosphorylation sites at the N-terminus. *In vitro* binding experiments showed the N-terminal region of IRBIT to be essential for interaction, and the IRBIT-binding region of IP_3R1 was mapped to the IP_3-binding core. IP_3 dissociated IRBIT from IP3R1 with an EC_{50} of approx. 0.5 μM, i.e. it was 50 times more potent than other inositol polyphosphates. Moreover, alkaline phosphatase treatment abolished the interaction, suggesting that the interaction was dualistically regulated by IP_3 and phosphorylation. Immunohistochemical studies and co-immunoprecipitation assays showed the relevance of the interaction in a physiological context. These results suggest that IRBIT is released from activated IP_3R, raising the possibility that IRBIT acts as a signalling molecule downstream from IP_3R.

Actually, the downstream target of IRBIT is pNBC1 (pancreas-type Na^+/HCO_3^- cotransporter 1) and IRBIT activates pNBC1 to regulate acid–base balance [37a].

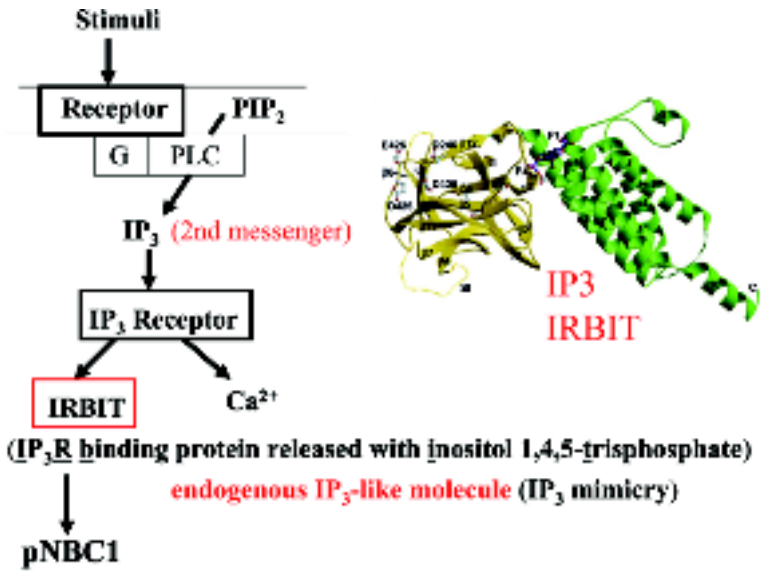

Figure 4 The role of IP_3 is not only to release Ca^{2+} but also to release IRBIT.

CARP

CARP was identified as one of the Purkinje-cell-specific genes [38]. CARP is composed of 291 amino acids, but lacks carbonic anhydrase activity due to the absence of catalytic zinc-co-ordinating residues [39]. CARP has been identified by the yeast two-hybrid system to bind to the modulatory domain of IP_3R1 (amino acids 1387–1647) [32]. CARP inhibits IP_3 binding to IP_3R1 by reducing the affinity for IP_3. IP_3 sensitivity for IICR in Purkinje cells is low compared with other tissues. This unique feature could be due to co-expression of CARP in Purkinje cells and its inhibitory effects on IP_3 binding of the IP_3R.

ERp44

We found that ERp44, an ER luminal protein of the thioredoxin family, directly interacts with the third luminal loop of IP_3R1. The interaction requires a low ER Ca^{2+} level and the presence of luminal cysteine residues in their reduced form [40] (Figure 5). Ca^{2+} imaging experiments and single-channel recording of IP_3R1 activity with a planar lipid bilayer system demonstrated that IP_3R1 is directly inhibited by ERp44. Also, ERp44 overexpression protected the cells against apoptosis, showing the significance of Ca^{2+} release via IP_3R1 in regulating apoptosis. Thus ERp44 senses the environment in the ER lumen and modulates IP_3R1 activity accordingly, which should in turn contribute to regulating both intralumenal conditions and the complex patterns of cytosolic Ca^{2+} concentrations.

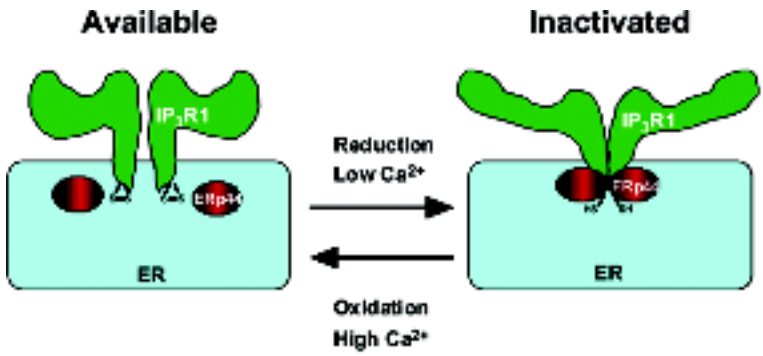

Figure 5 A new redox sensor in the ER regulates Ca^{2+} release. ERp44 (the thioredoxin family) senses the oxidoreduction state in the ER lumen and regulates IP_3R1 activity in a Ca^{2+}-dependent manner [40]. (i) Cysteine residues of 1L3V are required for inhibition of IP_3R1 by ERp44. (ii) Knockdown of ERp44 augments IICR in HeLa cells. (iii) ERp44 inactivates IP3R1 activity in the luminal redox in a Ca^{2+}-dependent manner.

IP_3R2 and IP_3R3 are essential for exocrine secretion

To evaluate the physiological roles of IP_3Rs, IP_3R2 and IP_3R3, we generated mice lacking genes for these intracellular Ca^{2+} release channels [41]. Mice with single gene disruption did not show any distinct phenotype at least for several months after birth, whereas double gene knockout mice died of starvation within 1 week following the end of the weaning period. The double mutant mice failed to switch to a dry food diet, but a diet of wet mashed food could rescue these mice from starvation. In accordance with this phenotype, both pilocarpine-induced saliva secretion and acetylcholine-activated Ca^{2+} signalling in submandibular acinar cells, the signalling cascade responsible for fluid secretion, were severely impaired in the double knockout mice. These results demonstrate an indispensable role of IP_3R2 and IP_3R3 in saliva secretion to tolerate solid food.

Another finding came from histological analysis of the knockout mice. In double mutants, zymogen granules accumulated in the cytosol of pancreatic acinar cells, and the *in vitro* experiment using dissociated acinar cells demonstrated that secretion of digestive enzymes (such as amylase and lipase) in response to muscarinic acetylcholine receptor stimulation, was abolished [41]. These results show that IP_3R2 and IP_3R3, co-localized in the extreme apical regions of acinar cells, play crucial roles in exocrine function of the pancreas. Despite approximately equal caloric intake, double mutants had reduced body weights and lower blood glucose levels than their wild-type littermates. It is hypothesized that defects in digestion could account for the malnourishment seen in these mice.

We also found that IP_3R2 and IP_3R3 were involved in brain development. During the specific period (after postnatal day 12) in the postnatal development of the cerebellum, more cells were found to be present in the cerebellar external granular layer in double mutants than littermate control animals (A. Futatsugi, E. Ebisui and K. Mikoshiba, unpublished work). Taken together, these results

show that IP_3R2 and IP_3R3, having some degree of functional redundancy, play critical roles in physiologically important phenomena such as exocrine function of the salivary gland and the pancreas, as well as brain development.

Ca^{2+} dynamics in cerebellar Purkinje cells

Ca^{2+} and Na^+ play important roles in neurons, such as in synaptic plasticity. Their concentrations in neurons change dynamically in response to synaptic inputs, but their kinetics have not been compared directly. We investigated the mechanisms and dynamics of Ca^{2+} and Na^+ transients by simultaneous monitoring in Purkinje cell dendrites in mouse cerebellar slices [42]. High-frequency parallel fibre stimulation (50 Hz, 350 times) depolarized Purkinje cells, and Ca^{2+} transients were observed at the anatomically expected sites. The magnitude of the Ca^{2+} transients increased linearly with increasing numbers of parallel fibre inputs. With 50 stimuli, Ca^{2+} transients lasted for seconds, and the peak Ca^{2+} concentration reached 100 μM, which was much higher than that reported previously, although it was still confined to a part of the dendrite. In contrast, Na^+ transients were sustained for tens of seconds and diffused away from the stimulated site. Pharmacological interventions revealed that Na^+ influx through AMPA (α-amino-3-hydroxy-5-methylisoxazole-4-propionic acid) receptors and Ca^{2+} influx through P-type Ca^{2+} channels were essential players, that AMPA receptors did not operate as a Ca^{2+} influx pathway and that Ca^{2+} release from intracellular stores through IP_3Rs or ryanodine receptors did not contribute greatly to the large Ca^{2+} transients.

Amplification of Ca^{2+} signalling by diacylglycerol-mediated IP_3 production

Various hormonal stimuli and growth factors activate the mammalian TRPC (canonical transient receptor potential) channel through phospholipase C activation. However, the precise mechanism of the regulation of the TRPC channel activity remains unknown. We provide the first evidence that direct tyrosine phosphorylation by Src family PTKs (protein tyrosine kinases) is a novel mechanism for modulating TRPC6 channel activity. We found that TRPC6 is tyrosine-phosphorylated in COS-7 cells when co-expressed with Fyn, a member of the Src family PTKs [43]. We also found that Fyn interacts with TRPC6 and that the interaction is mediated by the SH2 (Src homology 2) domain of Fyn and the N-terminal region of TRPC6 in a phosphorylation-independent manner. In addition, we have demonstrated the physical association of TRPC6 with Fyn in the mammalian brain. Moreover, we have shown that stimulation of the epidermal growth factor receptor induced rapid tyrosine phosphorylation of TRPC6 in COS-7 cells. This epidermal growth factor-induced tyrosine phosphorylation of TRPC6 was significantly blocked by PP2, a specific inhibitor of Src family PTKs, and by a dominant-negative form of Fyn, suggesting that the direct phosphorylation of TRPC6 by Src family PTKs could be caused by

physiological stimulation. Furthermore, using single-channel recording, we showed that Fyn modulates TRPC6 channel activity via tyrosine phosphorylation. Thus our findings demonstrated that tyrosine phosphorylation by Src family PTKs is a novel regulatory mechanism of TRPC6 channel activity.

An RNA-interacting protein, SYNCRIP, and mRNA transport

mRNA transport and local translation in the neuronal dendrite is implicated in the induction of synaptic plasticity. We have cloned an RNA-interacting protein, SYNCRIP (heterogeneous nuclear ribonuclear protein Q1/NSAP1), that is suggested to be important for the stabilization of mRNA [44]. We have reported that SYNCRIP is a component of mRNA granules in rat hippocampal neurons [45]. SYNCRIP was mainly found at cell bodies, but punctate expression patterns in the proximal dendrite were also seen. Time-lapse analysis in living neurons revealed that the granules labelled with fluorescent protein-tagged SYNCRIP were transported bi-directionally within the dendrite at approx. 0.05 μm/s. Treatment of neurons with nocodazole significantly inhibited the movement of GFP–SYNCRIP-positive granules, indicating that the transport of SYNCRIP-containing granules is dependent on microtubules. The distribution of SYNCRIP-containing granules overlapped with that of dendritic RNAs and elongation factor 1α. SYNCRIP was also found to be co-transported with GFP-tagged human staufen 1 and the 3′-untranslated region of IP_3R1 mRNA. These results suggest that SYNCRIP is transported within the dendrite as a component of mRNA granules and raises the possibility that mRNA turnover in mRNA granules and the regulation of local protein synthesis in neuronal dendrites may involve SYNCRIP.

Dynamic visualization of IP_3R1 by AFM (atomic force microscopy)

The EM images were obtained from static specimens in a vacuum. Dynamic aspects of the conformational change have never been visualized in a natural environment. We attempted to observe the structure of the receptor on a biological membrane by AFM. AFM can be used to study samples in solution, which may represent a natural environment. AFM revealed a globular structure on the purified ER membrane, which was identified to be the cytosolic domain of IP_3R1 by monoclonal antibody and EM [46]. The authentic IP_3R1, which was immunopurified from mouse cerebella had about the same dimensions with those of the protrusion found on the membrane. Establishing an AFM observation technique for biological samples will add a new dimension to the analysis of the structure–function relationships of membrane proteins.

References

1. Streb, H., Irvine, R.F., Berridge, M.J. and Schulz, I. (1983) Nature **306**, 67–69
2. Snyder, S.H., Sabatini, D.M., Lai, M.M., Steiner, J.P., Hamilton, G.S. and Suzdak, P.D. (1998) Trends Pharmacol. Sci. **19**, 21–26
3. Sudhof, T.C., Newton, C.L., Archer, B.T.D., Ushkaryov, Y.A. and Mignery, G.A. (1991) EMBO J. **10**, 3199–3206
4. Maeda, N., Wada, K., Yuzaki, M. and Mikoshiba, K. (1989) Brain Res. **489**, 21–30
5. Mikoshiba, K., Nagaike, K., Aoki, E. and Tsukada, Y. (1979) Brain Res. **177**, 287–299
6. Maeda, N., Niinobe, M., Nakahira, K. and Mikoshiba, K. (1988) J. Neurochem. **51**, 1724–1730
7. Maeda, N., Niinobe, M. and Nikoshiba, K. (1990) EMBO J. **9**, 61–67
8. Furuichi, T., Yoshikawa, S., Miyawaki, A., Wada, K., Maeda, N. and Mikoshiba, K. (1989) Nature **342**, 32–38
9. Maeda, N., Kawasaki, T., Nakade, S., Yokota, N., Taguchi, T., Kasai, M. and Mikoshiba (1991) J. Biol. Chem. **266**, 1109–1116
10. Hirota, J., Michikawa, T., Miyawaki, A., Furuichi, T., Okura, I. and Mikoshiba, K. (1995) J. Biol. Chem. **270**, 19046–19051
11. Ferris, C.D., Huganir, R.L. and Snyder, S.H. (1990) Proc. Natl. Acad. Sci. U.S.A. **87**, 2147–2151
12. Miyawaki, A., Furuichi, T., Maeda, N. and Mikoshiba, K. (1990) Neuron **5**, 11–18
13. Kume, S., Muto, A., Inoue, T., Suga, K., Okano, H. and Mikoshiba, K. (1997) Science **278**, 1940–1943
14. Saneyoshi, T., Kume, S., Amasaki, Y. and Mikoshiba, K. (2002) Nature **417**, 295–299
15. Takei, K., Shin, R.M., Inoue, T., Kato, K. and Mikoshiba, K. (1998) Science **282**, 1705–1708
16. Matsumoto, M., Nakagawa, T., Inoue, T., Nagata, E., Tanaka, K., Takano, H., Minowa, O., Kuno, J. Sakakibara, S., Yamada, M. et al. (1996) Nature **379**, 168–171
17. Inoue, T., Kato, K., Kohda, K. and Mikoshiba, K. (1998) J. Neurosci. **18**, 5366–5373
18. Fujii, S., Matsumoto, M., Igarashi, K., Kato, H. and Mikoshiba, K. (2000) Learn. Mem. **7**, 312–320
19. Taufiq, A.M., Fujii, S., Yamazaki, Y., Sasaki, H., Kaneko, K., Li, J., Kato, H. and Mikoshiba, K. (2005) Learn. Mem. **12**, 594–600
20. Nishiyama, M., Hong, K., Mikoshiba, K., Poo, M.M. and Kato, K. (2000) Nature **408**, 584–588
21. Yamamoto-Hino, M., Sugiyama, T., Hikichi, K., Mattei, M.G., Hasegawa, K., Sekine, S., Sakurada, K., Miyawaki, A., Furuichi, T., Hasegawa, M. and Mikoshiba, K. (1994) Recept. Channels **2**, 9–22
22. Iwai, M., Tateishi, Y., Hattori, M., Mizutani, A., Nakamura, T., Futatsugi, A., Inoue, T., Furuichi, T., Michikawa, T. and Mikoshiba, K. (2005) J. Biol. Chem. **280**, 10305–10317

22a. Yoshikawa, F., Iwasaki, H., Michikawa, T., Furuichi, T. and Mikoshiba, K. (1999) J. Biol. Chem. **274**, 328–334

22b. Uchida, K., Miyauchi, H., Furuichi, T., Michikawa, T. and Mikoshiba, K. (2003) J. Biol. Chem. **278**, 16551–16560

23. Tateishi, Y., Hattori, M., Nakayama, T., Iwai, M., Bannai, H., Nakamura, T., Michikawa, T., Inoue, T. and Mikoshiba, K. (2005) J. Biol. Chem. **280**, 6816–6822
24. Bosanac, I., Alattia, J.R., Mal, T.K., Chan, J., Talarico, S., Tong, F.K., Tong, K.I., Yoshikawa, F., Furuichi, T., Iwai, M. et al. (2002) Nature **420**, 696–700
25. Bosanac, I., Yamazaki, H., Matsu-Ura, T., Michikawa, T., Mikoshiba, K. and Ikura, M. (2005) Mol. Cell **17**, 193–203
26. Hamada, K., Terauchi, A. and Mikoshiba, K. (2003) J. Biol. Chem. **278**, 52881–52889
27. Hamada, K., Miyata, T., Mayanagi, K., Hirota, J. and Mikoshiba, K. (2002) J. Biol. Chem. **277**, 21115–21118
28. Sato, C., Hamada, K., Ogura, T., Miyazawa, A., Iwasaki, K., Hiroaki, Y., Tani, K., Terauchi, A., Fujiyoshi, Y. and Mikoshiba, K. (2004) J. Mol. Biol. **336**, 155–164

28a. Bosanac, I., Michikawa, T., Mikoshiba, K. and Ikura, M. (2004) Biochim. Biophys. Acta **1742**, 89–102

29. Bannai, H., Inoue, T., Nakayama, T., Hattori, M. and Mikoshiba, K. (2004) J. Cell Sci. **117**, 163–175
30. Tang, T.S., Tu, H., Chan, E.Y., Maximov, A., Wang, Z., Wellington, C.L., Hayden, M.R. and Bezprozvanny, I. (2003) Neuron **39**, 227–239

31. Yoo, S.H., So, S.H., Kweon, H.S., Lee, J.S., Kang, M.K. and Jeon, C.J. (2000) J. Biol. Chem. **275**, 12553–12559
32. Hirota, J., Ando, H., Hamada, K. and Mikoshiba, K. (2003) Biochem. J. **372**, 435–441
33. Tu, J.C., Xiao, B., Yuan, J.P., Lanahan, A.A., Leoffert, K., Li, M., Linden, D.J. and Worley, P.F. (1998) Neuron **21**, 717–726
34. Zhang, S., Mizutani, A., Hisatsune, C., Higo, T., Bannai, H., Nakayama, T., Hattori, M. and Mikoshiba, K. (2003) J. Biol. Chem. **278**, 4048–4056
35. Bourguignon, L.Y. and Jin, H. (1995) J. Biol. Chem. **270**, 7257–7260
36. Ando, H., Mizutani, A., Matsu-Ura, T. and Mikoshiba, K. (2003) J. Biol. Chem. **278**, 10602–10612
37. Boehning, D., Patterson, R.L., Sedaghat, L., Glebova, N.O., Kurosaki, T. and Snyder, S.H. (2003) Nat. Cell Biol. **5**, 1051–1061
37a. Shirakabe, K., Priori, G., Yamada, H., Ando, H., Horita, S., Fujita, T., Fujimoto, I., Mizutani, A., Seki, A. and Mikoshiba, K. (2006) Proc. Natl. Acad. Sci. U.S.A. **103**, 9542–9547
37b. Ando, H., Mizutani, A., Kiefer, H., Tsuzurugi, K., Michikawa, T. and Mikoshiba, K. (2006) Mol. Cell **22**, 1–12
38. Nogradi, A., Jonsson, N., Walker, R., Caddy, K., Carter, N. and Kelly, C. (1997) Dev. Brain Res. **98**, 91–101
39. Kato, K. (1990) FEBS Lett. **271**, 137–140
40. Higo, T., Hattori, M., Nakamura, T., Natsume, T., Michikawa, T and Mikoshiba, K. (2005) Cell **120**, 85–98
41. Futatsugi, A., Nakamura, T. Yamada, M.K., Ebisui, E., Nakamura, K., Uchida, K., Kitaguchi, T., Takahashi-Iwanaga, H., Noda, T., Aruga, J. and Mikoshiba, K. (2005) Science **309**, 2232–2234
42. Kuruma, A., Inoue, T. and Mikoshiba, K. (2003) Eur. J. Neurosci. **18**, 2677–2689
43. Hisatsune, C., Nakamura, K., Kuroda, Y., Nakamura, T. and Mikoshiba, K. (2005) J. Biol. Chem. **280**, 11723–11730
44. Mizutani, A., Fukuda, M., Ibata, K., Shiraishi, Y. and Mikoshiba, K. (2000) J. Biol. Chem. **275**, 9823–9831
45. Bannai, H., Fukatsu, K., Mizutani, A., Natsume, T., Iemura, S., Ikegami, T., Inoue, T. and Mikoshiba, K. (2004) J. Biol. Chem. **279**, 53427–53434
46. Suhara, W., Kobayashi, M., Sagara, H., Hamada, K., Goto, T., Fujimoto, I., Torimitsu, K. and Mikoshiba, K. (2006) Neurosci. Lett. **391**, 102–107